

# We are IntechOpen, the world's leading publisher of Open Access books Built by scientists, for scientists

**4,800**

Open access books available

**122,000**

International authors and editors

**135M**

Downloads

Our authors are among the

**154**

Countries delivered to

**TOP 1%**

most cited scientists

**12.2%**

Contributors from top 500 universities



**WEB OF SCIENCE™**

Selection of our books indexed in the Book Citation Index  
in Web of Science™ Core Collection (BKCI)

Interested in publishing with us?  
Contact [book.department@intechopen.com](mailto:book.department@intechopen.com)

Numbers displayed above are based on latest data collected.

For more information visit [www.intechopen.com](http://www.intechopen.com)



## Satellite coverage optimization problems with shaped reflector antennas

Adriano C. Lisboa and Douglas A. G. Vieira  
*ENACOM - Handcrafted Technologies*  
Brazil

Rodney R. Saldanha  
*Universidade Federal de Minas Gerais*  
Brazil

This chapter is devoted to optimization formulations of satellite coverage problems and their solution. They are specially useful in satellite broadcasting applications, where the information goes from one to many. Due to distance from target and power supply constraints, highly directive efficient reflector antennas are the best choice. There are many possible optimization formulations for this problem, depending fundamentally on specifications and degrees of freedom in the system. Some specific coverage problems considering broadband, radiation pattern constraints and interference are presented, where the degrees of freedom are purely geometric.

### 1. Satellite coverage problems

A satellite coverage problem queries for antennas in geostationary orbit of a planet, as shown in the example in Fig. 1 for the Brazilian territory, whose radiation pattern over a target is as close as possible to a specification.

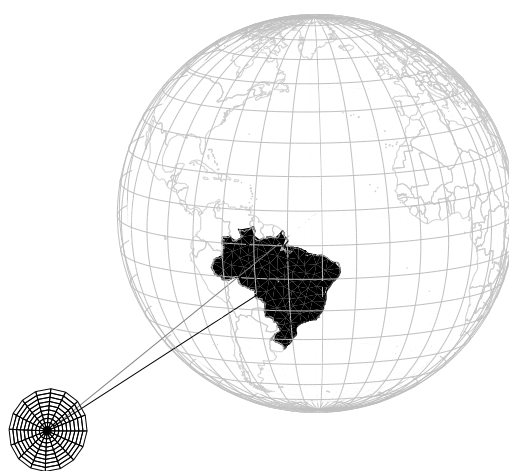


Fig. 1. Graphical illustration of a satellite coverage problem for the Brazilian territory.

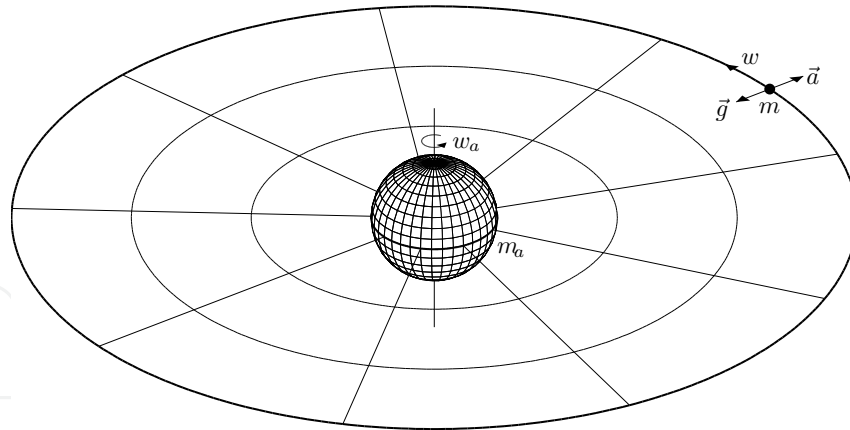


Fig. 2. Geostationary orbit (true scale) around a planet of mass  $m_a$  and angular speed  $w_a$ .

### 1.1 Satellite's orbit

Geosynchronous orbit is a requirement because it is considered a fixed target on the planet surface. Geostationary orbit (a special case of geosynchronous orbit) is a further requirement to reduce orbital station-keeping of the satellite. Geostationary means that the satellite centripetal force  $m\vec{a}$  and the planet gravitational force  $m\vec{g}$  are equal in modulus and opposite in direction (see Fig. 2), i.e.  $m\vec{a} = -m\vec{g}$ , where  $m$  is the satellite mass,  $\vec{a}$  is the satellite centripetal acceleration and  $\vec{g}$  is the planet gravitational acceleration. The direction constraint implies that the satellite is above the planet's equator. Using the notation  $\vec{a} = a\hat{a}$  to denote the modulus  $a = |\vec{a}|$  and unit direction  $\hat{a} = \vec{a}/|\vec{a}|$  of a vector  $\vec{a}$ , the modulus constraint implies  $ma = mg$ , where

$$a = w^2 r \quad (1)$$

$$g = \frac{Gm_a}{r^2} \quad (2)$$

where  $w$  is the satellite angular speed,  $G$  is the gravitational constant ( $G \approx 6.674 \times 10^{-11} \text{m}^3/\text{kg/s}^2$ ),  $m_a$  is the planet mass ( $m_a \approx 5.974 \times 10^{24} \text{kg}$  for Earth), and  $r$  is the distance from the planet center to the satellite, so that the geostationary orbit radius is given by

$$r_s = \sqrt[3]{\frac{Gm_a}{w_a^2}} \quad (3)$$

where  $w_a$  is the angular speed of the planet's rotation around its own axis ( $w_a \approx 7.292 \times 10^{-5} \text{rad/s}$  for Earth). The geostationary orbit radius depends only on planet properties. For Earth it is about  $42.2 \times 10^6 \text{m}$ .

### 1.2 Coordinate systems

A very important, yet simple, point in the mathematical model of the satellite is the definition of coordinate systems. In the context of satellite coverage problems, they can be defined by taking the planet, the antenna reflector or the antenna feed as reference. For now, consider planet coordinate system as any coordinate system that takes the planet center as its origin and the planet rotation axis as its z-axis.

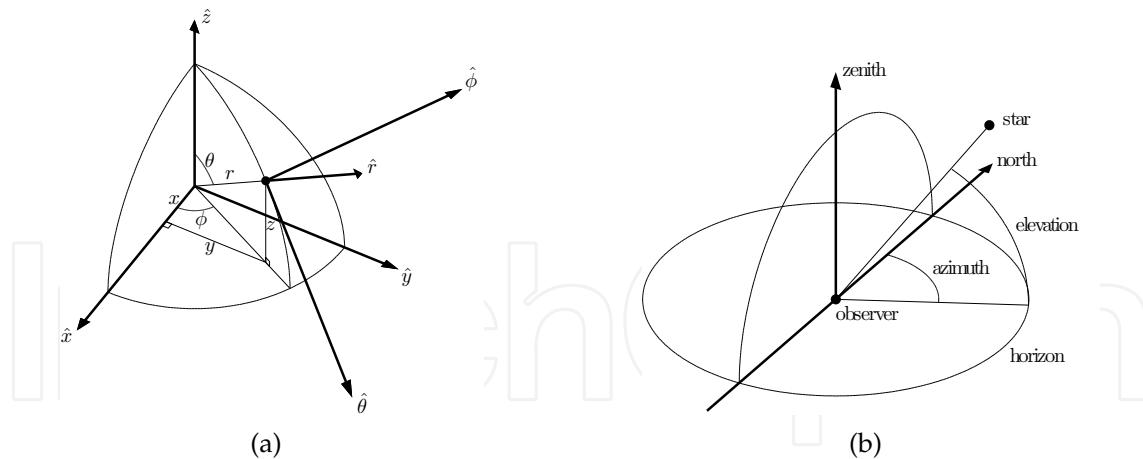


Fig. 3. Spherical coordinate system (a) and horizontal coordinate system (b).

Denote  $\vec{p} = x_p\hat{x} + y_p\hat{y} + z_p\hat{z}$  a point given in Cartesian coordinate system, and  $\vec{p} = r_p\hat{r} + \theta_p\hat{\theta} + \phi_p\hat{\phi}$  a point given in spherical coordinate system (see Fig. 3(a)), so that

$$\begin{aligned} x_p &= r_p \sin \theta_p \cos \phi_p \\ y_p &= r_p \sin \theta_p \sin \phi_p \\ z_p &= r_p \cos \theta_p \end{aligned} \quad (4)$$

Denote  $\vec{a} = a_x\hat{x} + a_y\hat{y} + a_z\hat{z}$  a vector given in Cartesian coordinate system, and  $\vec{a} = a_r\hat{r} + a_\theta\hat{\theta} + a_\phi\hat{\phi}$  a vector given in spherical coordinate system, so that

$$\begin{bmatrix} a_x \\ a_y \\ a_z \end{bmatrix} = \begin{bmatrix} \sin \theta \cos \phi & \cos \theta \cos \phi & -\sin \phi \\ \sin \theta \sin \phi & \cos \theta \sin \phi & \cos \phi \\ \cos \theta & -\sin \theta & 0 \end{bmatrix} \begin{bmatrix} a_r \\ a_\theta \\ a_\phi \end{bmatrix} \quad (5)$$

and, since the transformation matrix  $U$  is unitary (i.e.  $U^{-1} = U^T$ ),

$$\begin{bmatrix} a_r \\ a_\theta \\ a_\phi \end{bmatrix} = \begin{bmatrix} \sin \theta \cos \phi & \sin \theta \sin \phi & \cos \theta \\ \cos \theta \cos \phi & \cos \theta \sin \phi & -\sin \theta \\ -\sin \phi & \cos \phi & 0 \end{bmatrix} \begin{bmatrix} a_x \\ a_y \\ a_z \end{bmatrix} \quad (6)$$

where it is important to note that the vector components depends on the angular components  $\theta$  and  $\phi$  of the point where the vector itself is defined. Coherently to this, a vector field (e.g. electric field  $\vec{E}$  and current density  $\vec{J}$ ) is a function of the position where each vector is defined (e.g.  $\vec{E}(\vec{r})$  and  $\vec{J}(\vec{r}')$ , where  $\vec{r}$  is an observer point and  $\vec{r}'$  is a source point). Also because the transformation matrix is unitary, the modulus of a vector does not depend on which coordinate system it is evaluated: just take the square root of the sum of its squared components.

The horizontal coordinate system, as shown in Fig. 3(b), is slightly different. It is a kind of celestial coordinate system, where positions are mapped on a sphere centered in the observer, originally taking the north pole of Earth as origin and the zenith as reference. It is defined by two components: azimuth (horizontal angular distance to the north) and elevation (vertical angular distance to the ground). It is very convenient to map deviations around a direction and it will be used to map radiation patterns where the observer is the satellite.

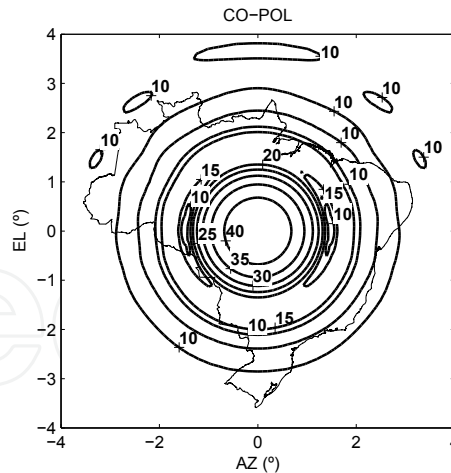


Fig. 4. Radiation pattern of a parabolic antenna illuminating the Brazilian territory. It is shown the level sets of the co-polarization gain (dBi) relative to an isotropic radiation in each direction given in reflector horizontal coordinate system.

### 1.3 Degrees of freedom in satellite's position and direction

Considering a geostationary orbit of radius  $r_s$  relative to the planet center, the remaining degree of freedom in the satellite position given in planet spherical coordinate system

$$\vec{p} = r_s \hat{r} + \frac{\pi}{2} \hat{\theta} + \phi_p \hat{\phi} \quad (7)$$

is its angular position  $\phi_p$  (it defines a location on the geostationary circle). The satellite is directed to a point on the planet surface

$$\vec{t} = r_a \hat{r} + \theta_t \hat{\theta} + \phi_t \hat{\phi} \quad (8)$$

where  $r_a$  is the planet radius ( $r_a \approx 6.4 \times 10^6$  m for Earth). The center of mass  $\vec{c}$  of the target is a good reference, as shown in Fig. 1, so that  $\theta_t = \theta_c$  and  $\phi_t = \phi_p = \phi_c$ . However, the degrees of freedom  $\phi_p$ ,  $\theta_t$  and  $\phi_t$  may be let as optimization variables for the satellite coverage problem.

### 1.4 Radiation pattern specification

A typical radiation pattern of a classical reflector antenna is shown in Fig. 4, where the target is the Brazilian territory. This highly directive pattern is desired for one-to-one communications (i.e. when target is a point), but can be improved when one-to-many communications (i.e. when target is an area) are considered. The most fair radiation pattern for broadcasting is the one that uniformly illuminates the target area, and only that. However different types of coverage can also be specified by gain lower or upper bounds, energy confinement inside target, radiation polarization or broadband operation.

## 2. Electromagnetic model

### 2.1 Antenna type selection

Since energy must be collimated within a few degrees around its main radiation direction, reflector antennas are very suitable and the natural choice.

A reflector antenna is composed by feed and reflector, as shown in Fig. 5. The main function of the feed is to supply energy. The main function of the reflector is to collimate energy.

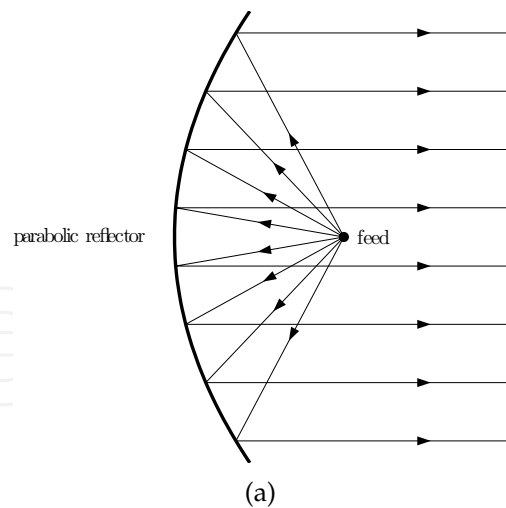


Fig. 5. Parabolic reflector antenna (a).

### 2.1.1 Parabolic reflector antenna

A point  $\vec{b} = (z, \rho)$  belongs to a parabola, as shown in Fig. 6, when it is at the same distance from the focus  $\vec{a} = (F, 0)$  and its projection  $\vec{c} = (-F, \rho)$  onto the directrix  $z = -F$ , which leads to the implicit equation

$$z = \frac{\rho^2}{4F} = \frac{x^2 + y^2}{4F} \quad (9)$$

where  $F$  is called the focal distance.

The unit normal vector to the parabola can be written as

$$\hat{n} = \frac{2F\hat{z} - \rho\hat{\rho}}{\sqrt{4F^2 + \rho^2}} = \frac{2F\hat{z} - x\hat{x} - y\hat{y}}{\sqrt{4F^2 + x^2 + y^2}} \quad (10)$$

The angle of the normal vector  $\hat{n}$  to  $\hat{z}$  is

$$\theta = \arctan\left(\frac{|\rho|}{2F}\right) = \arctan\left(\frac{\sqrt{x^2 + y^2}}{2F}\right) \quad (11)$$

The direction of a ray from the focus to a point on the parabola can be written as

$$\hat{d} = \frac{(z - F)\hat{z} + \rho\hat{\rho}}{z + F} \quad (12)$$

so that

$$\begin{aligned} -\hat{d} \cdot \hat{n} &= \frac{-2zF + 2F^2 + \rho^2}{(z + F)\sqrt{4F^2 + \rho^2}} = \frac{-2zF + 2F^2 + 4zF}{(z + F)\sqrt{4F^2 + \rho^2}} \\ &= \frac{2F}{\sqrt{4F^2 + \rho^2}} \\ &= \hat{n} \cdot \hat{z} \\ &= \cos \theta \end{aligned} \quad (13)$$

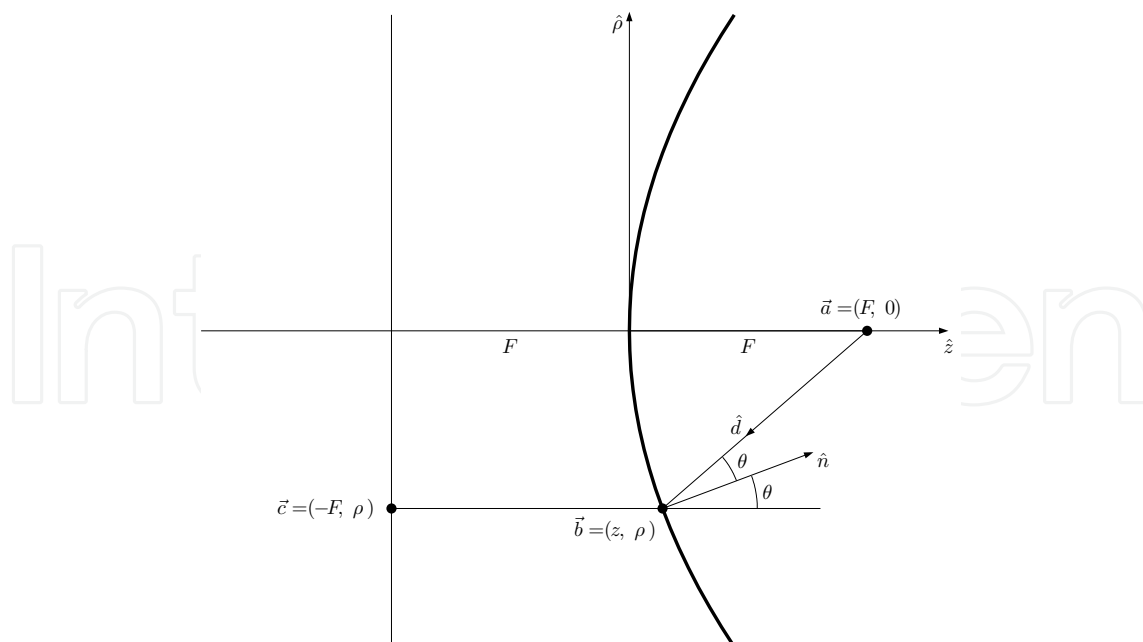


Fig. 6. Parabola with focus  $\vec{a} = (F, 0)$  and directrix  $z = -F$ , defined by points  $\vec{b} = (z, \rho)$ .

Hence, the angle between  $-\hat{d}$  and  $\hat{n}$  is the same as the angle between  $\hat{n}$  and  $\hat{z}$ . If the reflection is perfect (e.g. for electromagnetic waves reflector must be a perfect electric conductor), then  $\theta$  is the angle of reflection of the ray, which equals the angle of incidence, so that all reflected rays go towards  $\hat{z}$ .

A last notable feature of parabolic reflectors is that the distance traveled by two reflected rays originated from the focus up to a given  $z = z_a$  plane are exactly the same and valued to

$$\begin{aligned} |\vec{b} - \vec{a}| + z_a - z &= |\vec{b} - \vec{c}| + z_a - z \\ &= F + z + z_a - z \\ &= F + z_a \end{aligned} \quad (14)$$

Therefore, if all rays from the feed are in phase, then they will still be in phase after reflecting and reaching  $z = z_a$ . This is highly desired, considering that an aperture (i.e. a bounded region at a given  $z = z_a$ ) is most directive when the field distribution on it is uniform in phase and amplitude. Unfortunately, the same does not hold true for the amplitude, since the dispersive behavior from the feed up to the reflector attenuates non-uniformly each ray according to the respective distance  $F + z$ .

Fig. 7 shows a parabolic reflector antenna with circular aperture of radius  $R$ . The reflector center was displaced  $H$  towards  $\hat{y}$  together with a feed tilt of  $\tau$  in the  $x = 0$  plane, so that the feed do not block reflected waves.

## 2.2 Geometric parameterization of the antenna

In optimization, a parameterization that considers the expected configurations to meet specified requirements reduce the search space and, hence, the computational effort to solve the optimization problem.

For a single reflector antenna, the expected shape is nearly parabolic, convex, continuous and smooth. A suitable parameterization would be a set of basis functions capable to represent

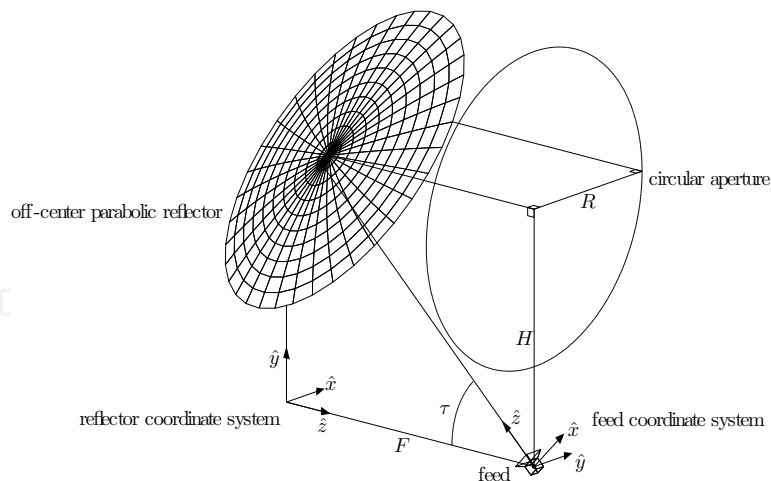


Fig. 7. Off-center parabolic reflector antenna.

any convex function, just like Fourier series are for periodic functions. Unfortunately, this is still an open problem. A parameterization that takes into consideration the expected shapes for a single reflector antenna is based on four triangular Bézier patches (Lisboa et al., 2006) to represent the reflector shape. Bézier patches are very common in computer aided geometric design. The shape of the object they represent is controlled by the position of vertices of a grid, called control points.

The feed position and direction can represent up to 5 geometric degrees of freedom for the antenna.

### 2.3 Electromagnetic analysis

In optimization, the antenna must be simulated (analysed) so that specified measures can be evaluated. These measures are evaluated at the so called observer points, denoted by  $\vec{r}$ . In spherical coordinates, observer points are written as  $\vec{r} = r\hat{r} + \theta\hat{\theta} + \phi\hat{\phi}$ . Analogously, source points are denoted by  $\vec{r}'$ .

Some key points concerning the electromagnetic model of the reflector antenna are depicted next.

#### 2.3.1 Harmonic fields

A very useful simplification in field propagation formulation is to consider harmonic components of it. This assumption allows to express the instantaneous field as the product of two terms: one depending only on space (i.e. amplitude, phase and direction at some spacial position) and another one depending only on time. The instantaneous field relative to a single harmonic component can be written as

$$\begin{aligned}\vec{E}(\vec{r}, t) &= \text{Re} \left( \vec{E}(\vec{r}) e^{j\omega t} \right) \\ &= \text{Re}(\vec{E}(\vec{r})) \cos(\omega t) - \text{Im}(\vec{E}(\vec{r})) \sin(\omega t) \\ &= \frac{1}{2} \left( \vec{E}(\vec{r}) e^{j\omega t} + \vec{E}^*(\vec{r}) e^{-j\omega t} \right)\end{aligned}\quad (15)$$

where  $t$  is the time,  $\vec{E}(\vec{r})$  is an harmonic field at angular frequency  $\omega = 2\pi\nu$ ,  $\nu$  is the frequency, and  $j$  is the imaginary unit. Since any time independent phase angle or attenuation could be



put into  $\vec{E}(\vec{r})$  (i.e.  $A e^{j\omega t + \alpha + j\beta} = A e^{\alpha} e^{j\beta} e^{j\omega t} = A' e^{j\omega t}$ ), they were set to zero. Analyzing field distributions at a single frequency (harmonic) is enough in many applications and, even if it is not, it may be possible to formulate a field distribution as a sum of harmonic components.

### 2.3.2 Feed model

The feed of a reflector antenna must radiate the energy that will be collimated by the reflector. It must be directive in order to waste less energy by missing the reflector.

One of the most simple mathematical feed model is the raised cosine, which can be written in feed coordinate system as

$$\vec{E}(\vec{r}) = \begin{cases} \frac{e^{-jkr}}{r} \cos^q \theta (\cos \phi \hat{\theta} - \sin \phi \hat{\phi}), & \theta \leq 90^\circ \\ 0, & \theta > 90^\circ \end{cases} \quad (16)$$

where  $q$  is an exponent that controls the feed directivity,  $k = w\sqrt{\mu\epsilon}$  is the wavenumber,  $\mu$  and  $\epsilon$  are the magnetic permeability and electric permittivity of free space, and  $j$  is the imaginary unit. Its simplicity allows some analytical analysis and its radiation pattern approximate real world feeds.

The raised cosine formulation is a typical far field equation: no field component towards  $\hat{r}$ , phase factor  $e^{-jkr}$ , and attenuation factor  $1/r$ . The remaining terms are related to field strength and polarization in each direction defined by  $\phi$  and  $\theta$ . Given the electric field  $\vec{E}(\vec{r})$  in free space at  $r \gg 1/k$ , the magnetic field  $\vec{H}(\vec{r})$  is given by

$$\vec{H}(\vec{r}) = \frac{1}{\eta} \hat{r} \times \vec{E}(\vec{r}) \quad (17)$$

where  $\eta$  is the intrinsic impedance of free space.

### 2.3.3 Radiated power

The electromagnetic power density is given by the Poynting vector

$$\begin{aligned} \vec{W}(\vec{r}, t) &= \vec{E}(\vec{r}, t) \times \vec{H}(\vec{r}, t) = \frac{1}{2} \left( \vec{E}(\vec{r}) e^{j\omega t} + \vec{E}^*(\vec{r}) e^{-j\omega t} \right) \times \frac{1}{2} \left( \vec{H}(\vec{r}) e^{j\omega t} + \vec{H}^*(\vec{r}) e^{-j\omega t} \right) \\ &= \frac{1}{2} \text{Re} \left( \vec{E}(\vec{r}) \times \vec{H}^*(\vec{r}) \right) + \frac{1}{2} \text{Re} \left( \vec{E}(\vec{r}) \times \vec{H}(\vec{r}) e^{j2\omega t} \right) \end{aligned} \quad (18)$$

where the first term independent on time  $t$  (mean power density) and the second term oscillates at  $2\omega$ .

The radiated power in free space of a source can be easier found by integrating the power density over a sphere in the far field region, where no field component towards  $\hat{r}$  is a good approximation. It can be written as

$$P_{rad} = \frac{1}{2} \oint_s \text{Re} \left( \vec{E}(\vec{r}) \times \vec{H}^*(\vec{r}) \right) \cdot d\vec{s} = \frac{1}{2\eta} \int_0^\pi \int_0^{2\pi} \left| \vec{E}(\vec{r}) \right|^2 r^2 \sin \theta d\phi d\theta \quad (19)$$

where  $s$  is a sphere of large radius and  $\eta$  is the intrinsic impedance of free space.

The radiated power of a raised cosine feed (16) is

$$\begin{aligned} P_{rad} &= \frac{1}{2\eta} \int_0^{\pi/2} \int_0^{2\pi} \frac{\cos^{2q} \theta}{r^2} r^2 \sin \theta d\phi d\theta = \frac{\pi}{\eta} \int_0^{\pi/2} \cos^{2q} \theta \sin \theta d\theta \\ &= \frac{\pi}{\eta(2q+1)} \end{aligned} \quad (20)$$

where  $q$  is the raised cosine exponent.

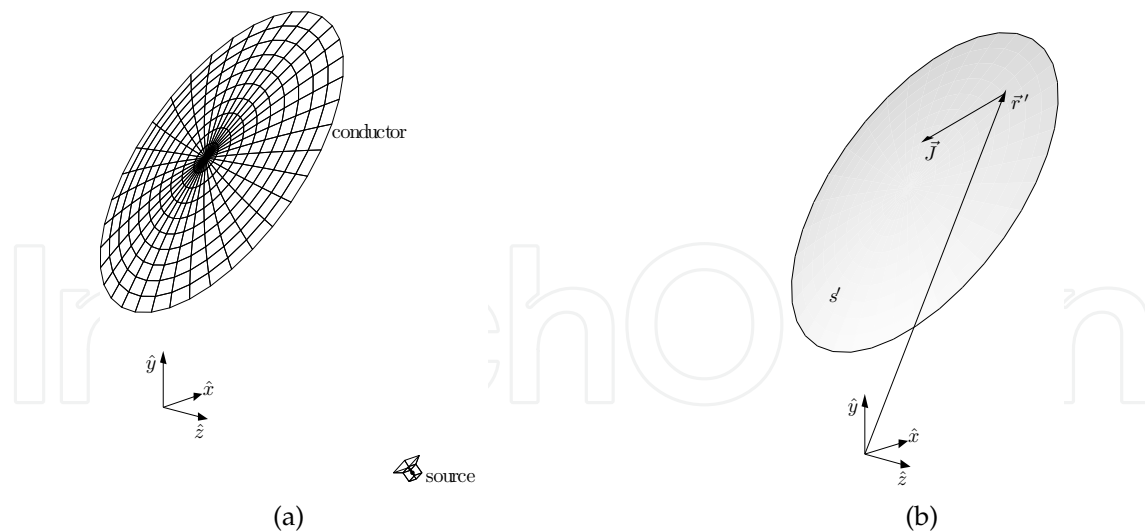


Fig. 8. Equivalence theorem: any field sources and scatters (a) can be replaced by equivalent current distributions (b).

### 2.3.4 Equivalent current sources

A common way to analyze reflector antennas is to replace the feed and reflectors (scatterers) by equivalent current sources, which is supported by the equivalence theorem (see Fig. 8). For a single, smooth and perfect electric conducting reflector, the physical optics approximation is accurate and can be written as

$$\vec{J}(\vec{r}') \approx 2\hat{n}(\vec{r}') \times \vec{H}_i(\vec{r}') \quad (21)$$

where  $\hat{n}$  is the unit normal vector at the source point  $\vec{r}'$ , and  $\vec{H}_i$  is the incident magnetic field at the source point  $\vec{r}'$ . Multiple reflectors may interact with each other, so that more complex procedures (e.g. method of moments) may have to be considered in order to determine accurate equivalent current sources.

### 2.3.5 Far field

Given a current density source  $\vec{J}(\vec{r}')$  over a surface  $s'$  in free space as shown in Fig. 9, the electric field can be accurately approximated for  $r \gg 1/k$  by the integral

$$\vec{E}(\vec{r}) = -j \frac{k\eta}{4\pi} \frac{e^{-jkr}}{r} \int_{s'} \left[ \vec{J}(\vec{r}') - (\vec{J}(\vec{r}') \cdot \hat{r}) \hat{r} \right] e^{jkr' \cdot \hat{r}} ds' \quad (22)$$

where  $k = \omega\sqrt{\mu\epsilon}$  is the wavenumber,  $\mu$  and  $\epsilon$  are the magnetic permeability and electric permittivity of free space,  $\eta$  is the intrinsic impedance of free space and  $j$  is the imaginary unit.

The far field integral can be evaluated by standard numerical methods (e.g. trapezoidal rule or Gaussian quadrature).

### 2.3.6 Definition of polarization

Polarization of a radiation is related to the orientation of the electric field. The third definition of Ludwig (1973) is very commonly used. It can be written as

$$E_{co}(\vec{r}) = \cos\phi E_\theta - \sin\phi E_\phi \quad (23)$$

$$E_{cx}(\vec{r}) = \sin\phi E_\theta + \cos\phi E_\phi \quad (24)$$



Fig. 9. Farfield  $\vec{E}$  at observer point  $\vec{r}$  relative to a current distribution  $\vec{J}$  at source points  $\vec{r}'$  over  $s'$ .

Note that the definition of co and cross polarization must be coherent to the feed radiation. For the raised cosine model (16), the field components in each polarization are

$$E_{co}(\vec{r}) = \frac{\cos^q \theta e^{-jkr}}{r} \quad (25)$$

$$E_{cx}(\vec{r}) = 0 \quad (26)$$

for  $\theta \leq 90^\circ$ . Unfortunately, reflectors may insert cross polarized components into the collimated field, even when the source does not radiate them.

### 2.3.7 Gain relative to an isotropic radiation

An isotropic radiation is the one that has the same intensity regardless of the direction. Hence, if an isotropic antenna radiates a power  $P_{rad}$ , the power density at a distance  $r$  away from it is

$$\vec{W}(\vec{r}) = \frac{P_{rad}}{4\pi r^2} \hat{r} \quad (27)$$

considering that  $P_{rad}$  is uniformly distributed over the area of an sphere of radius  $r$ .

The power density relative to an electric field  $\vec{E}$  in free space at  $r \gg 1/k$  away from the source is given by

$$\begin{aligned} \vec{W}(\vec{r}) &= \frac{1}{2} \text{Re} \left( \vec{E}(\vec{r}) \times \vec{H}^*(\vec{r}) \right) = \frac{1}{2\eta} \text{Re} \left( \vec{E}(\vec{r}) \times \hat{r} \times \vec{E}^*(\vec{r}) \right) \\ &= \frac{|\vec{E}(\vec{r})|^2}{2\eta} \hat{r} \end{aligned} \quad (28)$$

The gain relative to an isotropic radiation can be written as

$$G(\vec{r}) = \frac{W(\vec{r})}{\vec{W}(\vec{r})} = \frac{2\pi r^2 |\vec{E}(\vec{r})|^2}{\eta P_{rad}} \quad (29)$$

where  $P_{rad}$  is the feed radiated power and  $\eta$  is the intrinsic impedance of free space. When the gain is given in decibels (i.e.  $10 \log_{10} G$ ), the unit is called dBi to indicate that it is relative to an isotropic radiation.

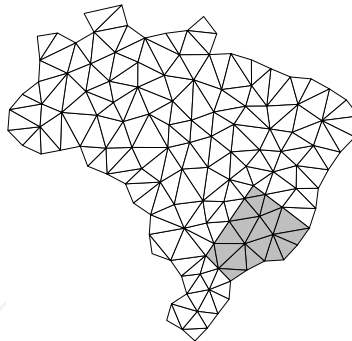


Fig. 10. Mesh over Brazilian territory used to define sample observer points.

### 3. Optimization problem formulations and solutions

#### 3.1 Sampling of observer points

To formulate optimization problems, sample observer points  $\vec{r}_i \in \mathbb{P}, i = 1, \dots, n_r$ , are uniformly spread all over the target. Fig. 10 shows a target instance, the Brazilian territory, where a triangular mesh is used to support the sampling. The antenna gain is evaluated in the vertices  $\mathbb{V} \subset \mathbb{P}$  for integrative measures (e.g. energy confinement) and in the centroids of triangles  $\mathbb{B} \subset \mathbb{P}$  for average measures (e.g. coverage). Subsets of samples can be differentiated to allow distinct specifications.

#### 3.2 Useful measures

##### 3.2.1 For coverage

A good measure of coverage is the average gain observed at the sample points. Considering the gain given in dB and that a maximum coverage is desired, an implicit uniformity measure is imbued in the average value.

##### 3.2.2 For energy confinement

Ideally, coverage also means energy confinement since illuminating a target implicitly means only that target. However, due to physical constraints, transition to outside regions is not discontinuous, so it is meaningful to formulate apart an energy confinement measure. The energy ratio inside the target can be numerically computed using the supporting mesh for sample observer points.

#### 3.3 Instance formulations of satellite coverage problems

The following instances of satellite coverage problems consider the Brazilian territory as target of a single feed single reflector antenna. The reference reflector is an off-center parabolic with circular aperture of radius  $R = 0.762\text{m}$ , focal distance  $F = 1.506\text{m}$ , and offset  $H = 1.245\text{m}$  along  $\hat{y}$  (Duan & Rahmat-Samii, 1995). The feed is modeled by a raised cosine radiation with exponent  $q = 14.28$  at frequency  $\nu = 11.95\text{GHz}$ , whose reference position is the reflector focus and reference direction is  $\tau = 42.77^\circ$  above the  $-z$ -axis on the  $x = 0$  plane (Duan & Rahmat-Samii, 1995). The satellite (reflector) is directed to the center of mass of the target. The reflector shape is parameterized by four triangular Bézier patches and the feed is parameterized by its position and direction on the plane  $x = 0$  of the reflector coordinate system (Lisboa et al., 2006). The number of design variables is  $n = 38$  and they compose the respective vector of design variables  $x \in \mathbb{R}^n$ . The sampling is supported by a mesh with 125 vertices  $\mathbb{V}$  and 190 triangle centroids  $\mathbb{B}$ , where 18 triangle centroids are labeled as southeast region  $\mathbb{B}'$ .

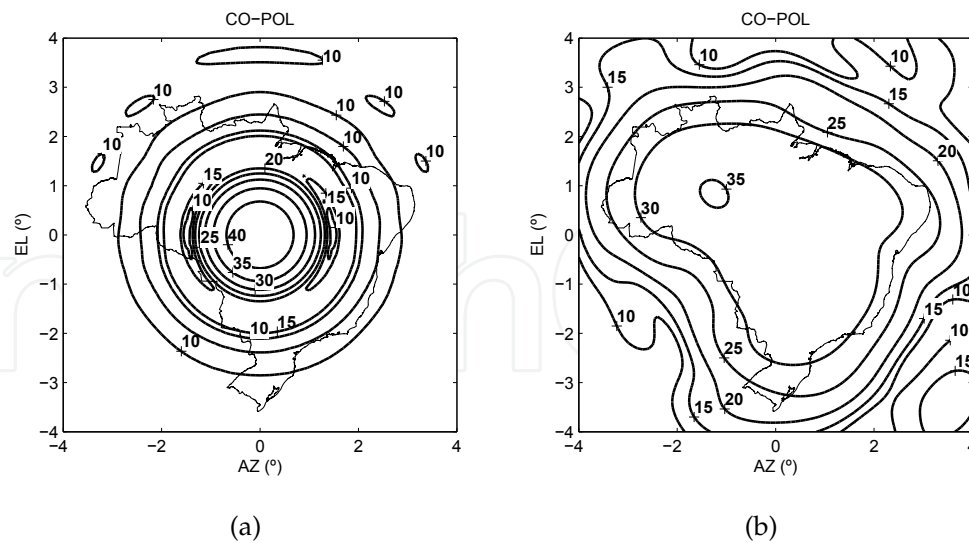


Fig. 11. Radiation patterns of the reference parabolic antenna (a) and of the optimal antenna for maximum uniform coverage (b).

Some instances of satellite coverage problems are shown next. Each one is intended to tackle a specific point on design of reflector antennas. Hence, the formulation techniques can be combined to produce more complete optimization problem formulations.

### 3.3.1 Maximum uniform coverage

The most simple satellite coverage problem aims to uniformly cover the target with the maximum energy possible. It can be formulated as the monoobjective optimization problem (Duan & Rahmat-Samii, 1995)

$$\text{minimize } f(x) = -\frac{1}{n_b} \sum_{i=1}^{n_b} 10 \log_{10} G(\vec{r}_i, x) \quad (30)$$

$$\text{subject to } x_{\min} \leq x \leq x_{\max} \quad (31)$$

where  $x \in \mathbb{R}^n$  is the vector of design variables,  $G$  is the antenna gain at an observer point  $\vec{r}$ , and  $\vec{r}_i \in \mathbb{B}$  denotes an observer point derived from triangle centroids.

The optimization algorithm iteratively queries the oracle of the optimization problem (antenna simulator in this case) with a vector of design variables  $x_k$  at iteration  $k$ , which in turn must answer with the respective values of the optimization functions at  $x_k$  (only  $f(x_k)$  in this case). Since the oracle query is expensive, the fewer iterations required for convergence, the better. Considering that the optimal antenna must still collimate energy since the target is far away, a highly directive classical reflector antenna is a good starting point.

Fig. 12 shows the optimal radiation pattern for maximum uniform coverage of the Brazilian territory (Lisboa et al., 2006). It was achieved by a search direction optimization algorithm with theoretical guarantees on improving the objective functions every iteration (Vieira, Takahashi & Saldanha, 2010), starting from a classical off-center parabolic reflector antenna.

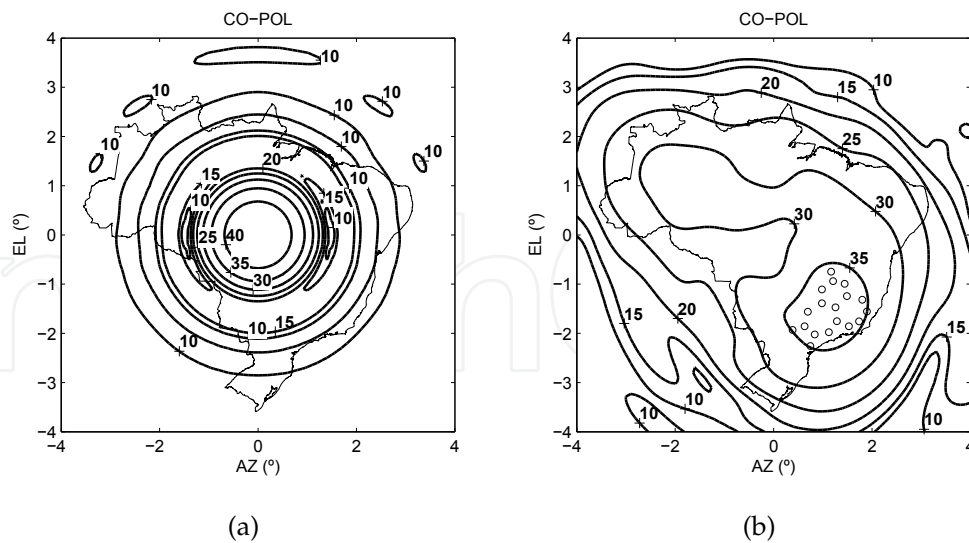


Fig. 12. Radiation patterns of the reference parabolic antenna (a) and of the optimal antenna for maximum uniform coverage constrained to lower bound of 35dBi in the southeast region (b).

### 3.3.1.1 Minimum gain constraints

To specify lower bounds of gain at subregions of the target, a subset of sample points can be used. It can be formulated as the monoobjective optimization problem (Vieira, Lisboa & Saldanha, 2010)

$$\text{minimize } f(x) = -\frac{1}{n_b} \sum_{i=1}^{n_b} 10 \log_{10} G(\vec{r}_i, x) \tag{32}$$

$$\text{subject to } g_j(x) = G_{\min,i} - G(\vec{r}_i, x) \leq 0, \forall \vec{r}_i \in \mathbb{B}' \subset \mathbb{B} \tag{33}$$

$$x_{\min} \leq x \leq x_{\max} \tag{34}$$

where  $x \in \mathbb{R}^n$  is the vector of design variables,  $G$  is the antenna gain at an observer point  $\vec{r}$ ,  $\vec{r}_i \in \mathbb{B}$  denotes an observer point derived from triangle centroids, and  $G_{\min,i}$  is the desired minimum gain at  $\vec{r}_i \in \mathbb{B}'$ . Each sample observer point inside the subregion  $\mathbb{B}'$  defines one constraint.

Fig. 12 shows the optimal radiation pattern for maximum coverage with a minimum gain 35dBi in the southeast region (Vieira, Lisboa & Saldanha, 2010), leading to a problem with 18 constraint functions. It was achieved by an ellipsoid method with an improved constraint functions treatment (Shor, 1977; Vieira, Lisboa & Saldanha, 2010; Yudin & Nemirovsky, 1977), starting from a classical off-center parabolic reflector antenna.

### 3.3.2 Maximum energy confinement

The search for maximum energy confinement can be formulated as the monoobjective optimization problem (Lisboa et al., 2008)

$$\text{minimize } f(x) = -\sum_{i=1}^{n_b} \frac{A_i}{4\pi r_a^2} \frac{1}{3} \sum_{j=1}^3 G(\vec{r}_{ij}, x) \tag{35}$$

$$\text{subject to } x_{\min} \leq x \leq x_{\max} \tag{36}$$

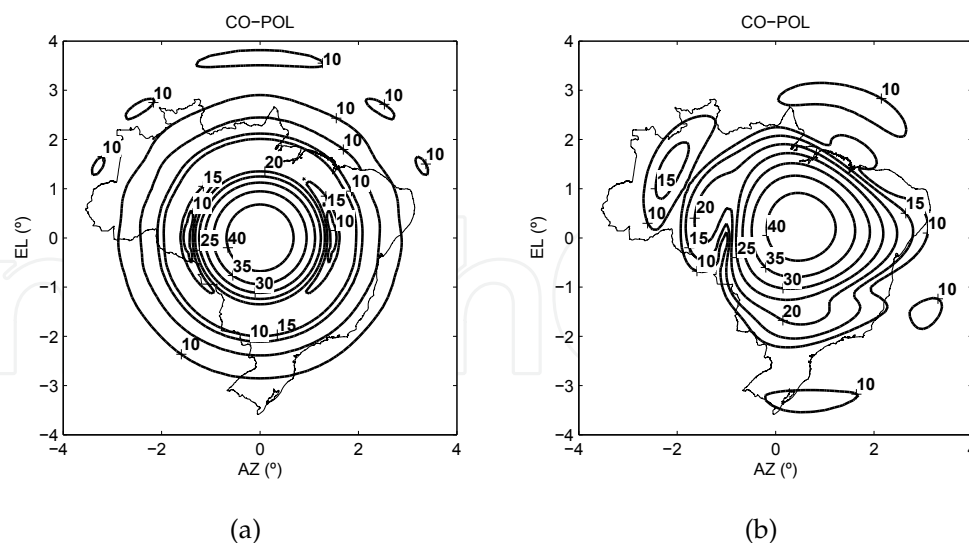


Fig. 13. Radiation patterns of the reference parabolic antenna (a) and of the optimal antenna for maximum energy confinement inside target area (b).

where  $x \in \mathbb{R}^n$  is the vector of design variables,  $G$  is the antenna gain at an observer point  $\vec{r}$ ,  $A$  is the area of triangles, and  $\vec{r}_{ij} \in \mathbb{V}$  is used to denote the  $j$ -th vertex of the  $i$ -th triangle.

Fig. 13 shows the optimal radiation pattern for maximum energy confinement inside target (Lisboa et al., 2008). It was achieved by a search direction optimization algorithm with theoretical guarantees on improving the objective functions every iteration (Vieira, Takahashi & Saldanha, 2010), starting from a classical off-center parabolic reflector antenna.

### 3.3.3 Maximum coverage and energy confinement

Optimal tradeoffs between maximum coverage and energy confinement can be formulated as the solution of the multiobjective optimization problem (Lisboa et al., 2008)

$$\text{minimize } f(x) = \begin{bmatrix} -\frac{1}{n_b} \sum_{i=1}^{n_b} 10 \log_{10} G(\vec{r}_i, x) \\ -\sum_{i=1}^{n_b} \frac{A_i}{4\pi r_a^2} \frac{1}{3} \sum_{j=1}^3 G(\vec{r}_{ij}, x) \end{bmatrix} \quad (37)$$

$$\text{subject to } x_{\min} \leq x \leq x_{\max} \quad (38)$$

where  $x \in \mathbb{R}^n$  is the vector of design variables,  $G$  is the antenna gain at an observer point  $\vec{r}$ ,  $A$  is the area of triangles,  $\vec{r}_i \in \mathbb{B}$  denotes an observer point derived from triangle centroids, and  $\vec{r}_{ij} \in \mathbb{V}$  is used to denote the  $j$ -th vertex of the  $i$ -th triangle.

Fig. 15 shows the optimal Pareto front for coverage and energy confinement for the Brazilian territory, whose respective radiation patterns of marked points are shown, from maximum coverage to maximum confinement, in Fig. 14(a), 14(b), 14(c) and 14(d). It was achieved by launching several times a search direction optimization algorithm with theoretical guarantees on improving all the objective functions every iteration (Vieira, Takahashi & Saldanha, 2010), starting from a classical off-center parabolic reflector antenna.

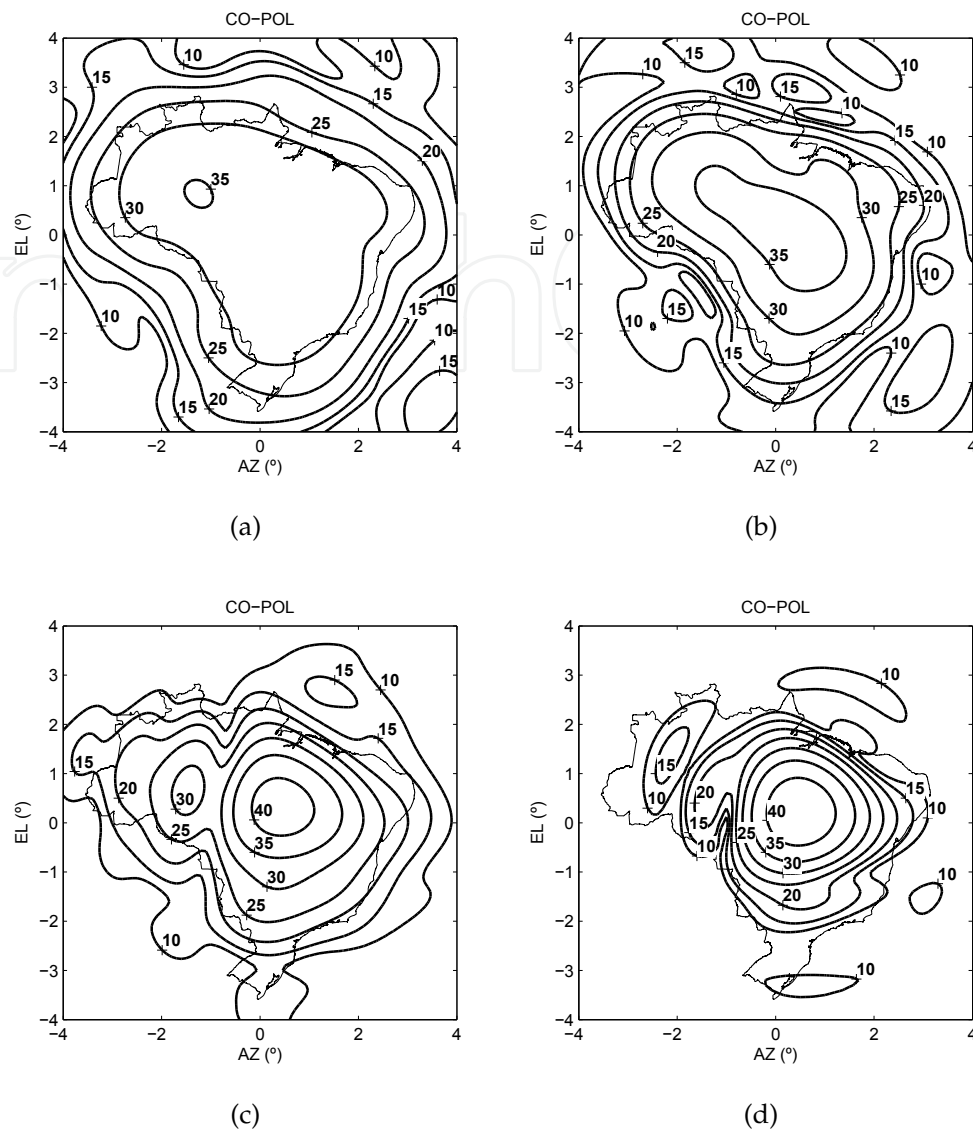


Fig. 14. Radiation patterns for maximum coverage (a), intermediate tradeoff for coverage and energy confinement (b-c), and for maximum energy confinement (d).

### 3.3.4 Broadband operation

To cope with broadband specifications, sample frequencies can be chosen inside the range so that the set of objective functions is considered for each sample frequency (Lisboa et al., 2006; 2008). For example, 5 sample frequencies for coverage and energy confinement lead to an optimization problem with 10 objective functions.

Another possible formulation is to take the worst case of each objective function inside the frequency range, which can be even more meaningful in practice. However, the convergence rate will be slower, considering that optimization algorithms that can directly cope with multiple objectives without any scalarization procedure (Vieira, Lisboa & Saldanha, 2010; Vieira, Takahashi & Saldanha, 2010) are faster when the number of objective functions increases. A final remark in this sense, is that the number of sample frequencies can be increased until it surpasses the number of design variables. From this point on, the Pareto set is likely to have



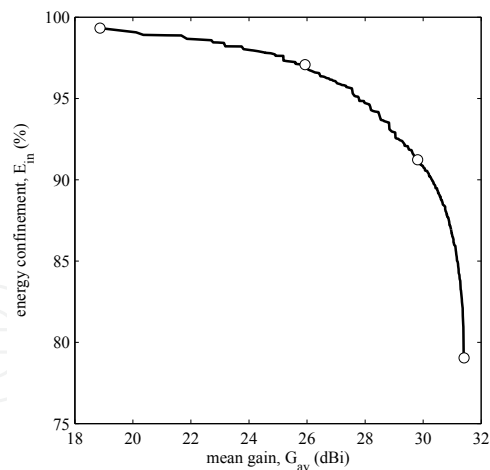


Fig. 15. Pareto front for coverage and energy confinement.

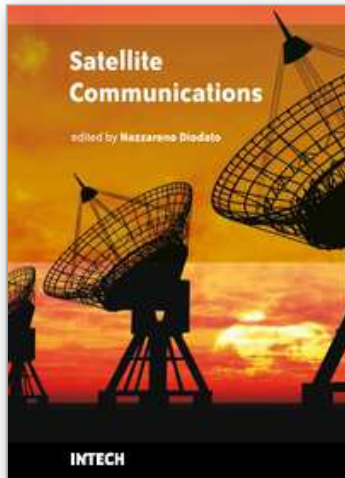
the same dimension of the search space, making numerically much easier to assert if a point is a local optimum.

#### Acknowledgements

This work was supported by FAPEMIG, CAPES and CNPq, Brazil.

#### 4. References

- Duan, D.-W. & Rahmat-Samii, Y. (1995). A generalized diffraction synthesis technique for high performance reflector antennas, *IEEE Transactions on Antennas and Propagation* **43**(1): 27–39.
- Lisboa, A. C., Vieira, D. A. G., Vasconcelos, J. A., Saldanha, R. R. & Takahashi, R. H. C. (2006). Multi-objective shape optimization of broad-band reflector antennas using the cone of efficient directions algorithm, *IEEE Transactions on Magnetics* **42**: 1223–1226.
- Lisboa, A. C., Vieira, D. A. G., Vasconcelos, J. A., Saldanha, R. R. & Takahashi, R. H. C. (2008). Decreasing interference in satellite broadband communication systems using modeled reflector antennas, *IEEE Transactions on Magnetics* **44**: 958–961.
- Ludwig, A. C. (1973). The definition of cross polarization, *IEEE Transactions on Antennas and Propagation* **21**(1): 116–119.
- Shor, N. Z. (1977). Cut-off method with space extension in convex programming problems, *Cybernetics* **12**: 94–96.
- Vieira, D. A. G., Lisboa, A. C. & Saldanha, R. R. (2010). An enhanced ellipsoid method for electromagnetic devices optimisation and design, *IEEE Transactions on Magnetics* (**accepted for publication**).
- Vieira, D. A. G., Takahashi, R. H. C. & Saldanha, R. R. (2010). Multicriteria optimization with a multiobjective golden section line search, *Mathematical Programming* **1-31**.
- Yudin, D. B. & Nemirovsky, A. S. (1977). Informational complexity and effective methods for solving convex extremum problems, *Matekon* **13**: 24–45.



## **Satellite Communications**

Edited by Nazzareno Diodato

ISBN 978-953-307-135-0

Hard cover, 530 pages

**Publisher** Sciyo

**Published online** 18, August, 2010

**Published in print edition** August, 2010

This study is motivated by the need to give the reader a broad view of the developments, key concepts, and technologies related to information society evolution, with a focus on the wireless communications and geoinformation technologies and their role in the environment. Giving perspective, it aims at assisting people active in the industry, the public sector, and Earth science fields as well, by providing a base for their continued work and thinking.

### **How to reference**

In order to correctly reference this scholarly work, feel free to copy and paste the following:

Adriano Lisboa, Douglas Vieira and Rodney Saldanha (2010). Satellite Coverage Optimization Problems with Shaped Reflector Antennas, *Satellite Communications*, Nazzareno Diodato (Ed.), ISBN: 978-953-307-135-0, InTech, Available from: <http://www.intechopen.com/books/satellite-communications/satellite-coverage-optimization-problems-with-shaped-reflector-antennas>

**INTECH**  
open science | open minds

### **InTech Europe**

University Campus STeP Ri  
Slavka Krautzeka 83/A  
51000 Rijeka, Croatia  
Phone: +385 (51) 770 447  
Fax: +385 (51) 686 166  
[www.intechopen.com](http://www.intechopen.com)

### **InTech China**

Unit 405, Office Block, Hotel Equatorial Shanghai  
No.65, Yan An Road (West), Shanghai, 200040, China  
中国上海市延安西路65号上海国际贵都大饭店办公楼405单元  
Phone: +86-21-62489820  
Fax: +86-21-62489821

© 2010 The Author(s). Licensee IntechOpen. This chapter is distributed under the terms of the [Creative Commons Attribution-NonCommercial-ShareAlike-3.0 License](https://creativecommons.org/licenses/by-nc-sa/3.0/), which permits use, distribution and reproduction for non-commercial purposes, provided the original is properly cited and derivative works building on this content are distributed under the same license.

IntechOpen

IntechOpen